Front. Earth Sci. China 2007, 1(3): 299–303
DOI 10.1007/s11707-007-0036-z

RESEARCH ARTICLE

Post-collisional adakitic biotite plagiogranites from Guangtoushan pluton (Mianxian, central China): Petrogenesis and tectonic implication

QIN Jiangfeng, LAI Shaocong (✉), LI Yongfei

State Key Laboratory of Continental Dynamics, Department of Geology, Northwest University, Xi'an 710069, China

Abstract The post-collisional Guangtoushan pluton intruded into the Mianlue suture, Central China. Geochemically, the Guangtoushan biotite plagiogranites show many close compositional similarities to high-silica adakites from the supra-subduction zone setting, but tend to have a higher concentration of K_2O (3.22%–3.84%). Chondrite-normalized rare earth element patterns are characterized by high ratios of $(La/Yb)_N$, concave-upward shapes of the heavy rare earth element (HREE), and a lack of significant Eu anomalies. In conjunction with high abundances of Ba and Sr, as well as low abundances of Y and HREE, these patterns suggest a feldspar-poor, garnet ± amohibole-rich fractionation mineral assemblage. Coupled with previous studies, we suggest that the Guangtoushan biotite plagiogranites were likely to be caused by subducting slab break-off during the late orogenic stage in the West Qinling orogenic belt.

Keywords Guangtoushan, biotite plagiogranite, adakite, petrogenesis, post-collision

1 Introduction

The eastern Asia continent is separated into the North and the South China blocks by the Qinling-Dabie orogenic belt. Therefore, it is very important to obtain accurate knowledge of the tectonics and evolution of the Qinling-Dabie orogenic belt to confirm the evolution of this continent (Lai et al., 2004; Sun et al., 2002; Zhang et al., 2002). In the western part of this orogenic belt, there is a ca. 400-km-long granitoid belt to the north of the Mianlue suture, roughly parallel to the suture (Fig. 1). According to regional geological observations, detailed petrological and zircon U-Pb chronology work, this granitoid belt is thought to be a "syn-collision" product (e.g. Sun et al., 2002; Zhang et al., 1994). Chronology and geochemistry of these granites can place effective constraints on the tectonic evolution of the Qinling orogenic belt.

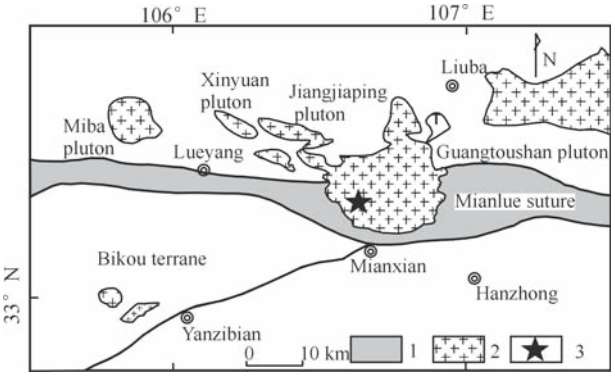

Fig. 1 Sketch map of Mesozoic granitoids to the north of Mianlue suture (revised from Zhang et al., 2001)
1) Mianlue ophiolite complex; 2) Indosinian granites; 3) Sampling locality

The present study focuses on the genesis of a post-orogenic high Sr/Y biotite plagiogranites from Guangtoushan pluton in South Qinling Mountains (Central China) (Fig. 1). The pluton is considered to be a product of collision between the Yangtze and North China terrains that resulted from closure of the Mianlue paleoocean. Based on field relations and petrological, geochemical characteristics documented in this study, the adakitic magma that formed the pluton is considered to have been generated by partial melting of mafic in lower crustal rocks at depths >45 km.

Translated from *Geological Bulletin of China*, 2007, 26(4): 466–471 [译自: 地质通报]

E-mail: shaocong@nwu.edu.cn

2 Geological setting

The ca. 400-km-long South Qinling granite belt trends almost parallel to the Mianlue suture in the west, to crops over an area of ca. 6 000 km^2 between the Daheba-Ningshan-Shanyang fault and to the Shangdan suture in the east. The age of the granitoids is between 205–220 Ma, indicating a syn-collision tectonic origin (e.g. Sun et al., 2002), and they have been classified on the basis of petrography and geochemistry into three suites: the Guangtoushan, Wulong and Dongjiangkou suites (Sun et al., 2002; Zhang et al., 1994).

The Guangtoushan pluton covers an area of ca. 900 km^2 and consists of two phases. The inner phase is mainly biotite granodiorite, and the outer phase in fine-grained biotite plagiogranite (Sun et al., 2002). The biotite plagiogranites are made up of plagioclase (50%–60%), K-feldspar (10%), quartz (15%–20%), and biotite ($\sim$10%). Accessory phases include zircon and apatite, allanite, clinozoisite and magnetite.

3 Major elements

Major elements of samples were determined by X-ray flouresence spectrometry with analytical errors less than 2%. Trace elements, including the rare earth element (REE), were analyzed by a Perkin-Elmer ELAN 6100 inductively coupled plasma source mass spectrometer (ICP-MS) at the State Key Laboratory of Continental Dynamics, Northwest University. Analytical errors for most elements are less than 2%. Major and trace element compositions of representative samples of the Guangtoushan biotite plagiogranites are listed in Table 1.

The rocks have 68.95%–71.93% SiO_2, 0.12%–0.36% TiO_2, high Al_2O_3 of (15.68%–16.72%) with A/CNK (molar $Al_2O_3/(CaO+K_2O+Na_2O)$) ranging from 1.00 to 1.02, indicating that they are metaluminous-aluminous (Fig. 2) with Na_2O = 4.67%–5.70%, K_2O = 2.12%–3.72%, Na_2O/K_2O = 1.26–1.52, MgO = 0.27%–0.46%. In terms of Na_2O versus K_2O, the biotite plagiogranites plot within the field of I-type granites (Fig. 3).

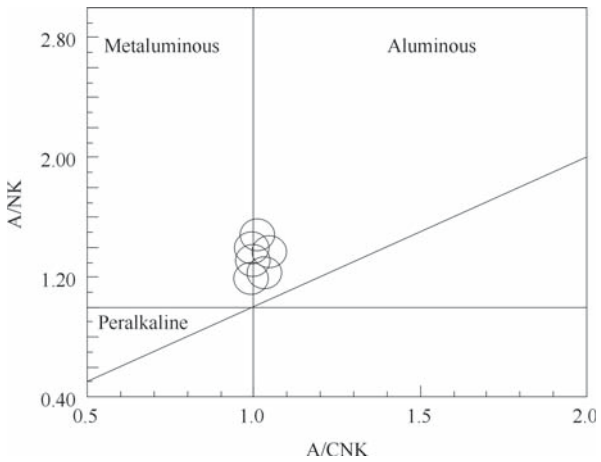

Fig. 2 Diagram of A/CNK-A/NK for the Guangtoushan biotite plagiogranites

Table 1 The analytical results of major (%) and trace element (μg/g) for the Guangtoushan granite

Sample	GTSG-02	GTSG-03	GTSG-04	GTSG-06	GTSG-10	GTSG-11
Rock	Biotite plagiogranites					
SiO_2	70.42	71.07	71.93	69.99	68.95	71.12
TiO_2	0.23	0.12	0.15	0.24	0.36	0.2
Al_2O_3	15.85	16.72	15.64	15.74	16.23	15.68
Fe_2O_3T	1.57	0.83	1.45	1.76	2.21	1.53
MnO	0.02	0.01	0.03	0.03	0.02	0.03
MgO	0.42	0.27	0.34	0.42	0.46	0.29
CaO	2.46	2.76	2.12	2.24	2.59	2
Na_2O	4.72	5.7	4.85	4.83	4.88	4.67
K_2O	3.11	2.12	3.36	3.46	3.21	3.72
P_2O_5	0.07	0.05	0.05	0.08	0.1	0.06
LOI	0.68	0.31	0.45	0.76	0.53	0.58
Total	99.55	99.96	100.37	99.55	99.54	99.88
A/CNK	1.01	1.00	1.01	0.99	1.00	1.02
σ	2.24	2.18	2.33	2.55	2.52	2.50
$Mg^{\#}$	34.85	39.42	31.92	32.31	29.39	27.49
Ba	1278	937	1149	1228	1581	1237
Rb	79.37	47.32	82.10	93.13	85.86	92.65
Sr	772.71	1052.85	805.34	731.28	903.87	704.61
Y	8.90	3.74	7.37	9.05	9.68	7.17
Zr	142.95	102.98	122.31	164.43	211.62	138.15
Nb	5.66	3.14	4.73	7.60	9.40	6.19
Th	6.374	1.52	6.25	10.65	11.01	8.38
Pb	12.28	11.10	20.18	15.09	16.35	15.12
Ga	18.7	17.1	18.4	19.0	19.0	19.3
Zn	47.1	31.2	61.4	47.3	44.8	42.2
Cu	4.26	4.29	4.63	4.93	11.2	4.69
Ni	2.26	2.09	2.29	2.01	2.12	2.06
V	14.7	9.74	13.0	14.0	23.4	12.1
Cr	2.51	2.15	2.41	1.92	2.10	2.05
Hf	3.49	2.60	3.39	4.18	4.95	3.58
Cs	1.17	0.69	1.06	1.32	1.43	1.32
Sc	2.23	1.37	1.96	2.29	2.06	1.99
Ta	0.63	0.36	0.52	0.61	0.70	0.64
Co	125	128	157	130	126	128
U	1.25	0.86	1.95	1.59	1.70	1.87
La	24.8	4.30	17.5	32.0	39.6	25.1
Ce	44.4	8.04	33.6	54.4	73.9	43.6
Pr	4.75	1.12	3.58	5.38	7.61	4.38
Nd	17.6	4.46	13.5	18.8	27.7	15.5
Sm	2.99	0.94	2.44	2.84	4.69	2.36
Eu	0.84	0.29	0.58	0.77	1.23	0.63
Gd	2.35	0.85	2.05	2.40	3.51	1.79
Tb	0.32	0.11	0.28	0.33	0.43	0.24
Dy	1.54	0.48	1.28	1.63	1.90	1.13
Ho	0.29	0.096	0.23	0.30	0.30	0.23
Er	0.74	0.23	0.63	0.78	0.70	0.59
Tm	0.11	0.044	0.10	0.12	0.096	0.095
Yb	0.63	0.20	0.58	0.65	0.47	0.51
Lu	0.10	0.040	0.10	0.10	0.072	0.086
Sr/Y	86.75	281.41	109.22	80.74	93.36	98.20
Y/Yb	14.21	18.77	12.77	13.97	20.50	14.02
La/Yb	39.55	21.60	30.32	49.32	83.77	49.10
δEu	0.93	0.97	0.76	0.88	0.89	0.907

Notes: $Mg^{\#} = Mg^{2+}/(Mg^{2+}+Fe^{2+}(total))*100$; $Fe^{2+}(total) = w\%(TFe_2O_3)/80$

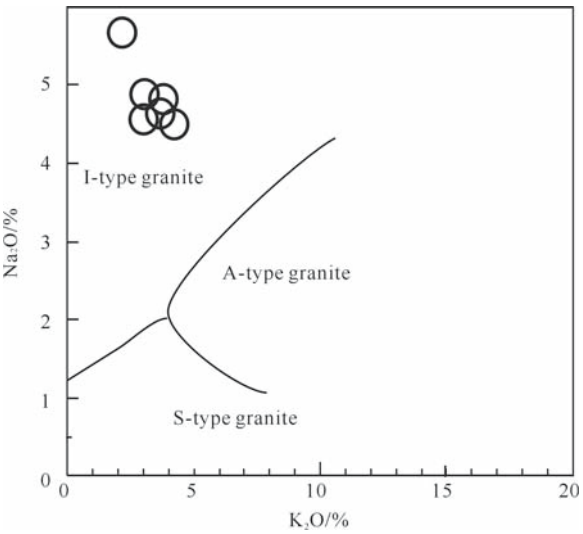

Fig. 3 Diagram of K_2O-Na_2O for the Guangtoushan biotite plagiogranites

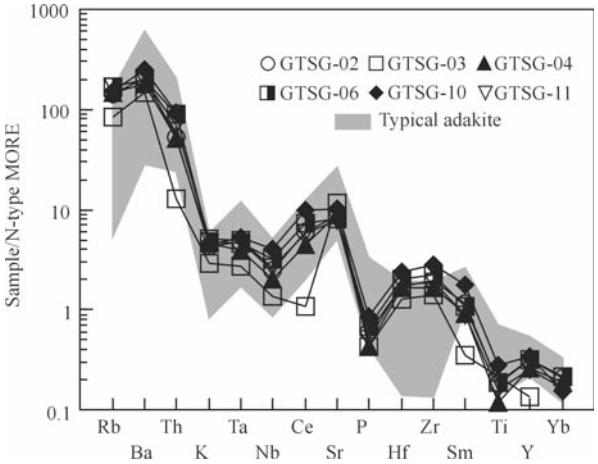

Fig. 5 Primitive mantle-normalized trace element concentrations of Guangtoushan granite
Normalized values are from Sun and McDonough (1989). Pattern of typical adakite is from Zhang et al. (2001)

4 Trace and rare earth elements

Trace element data show that the Guangtoushan biotite plagiogranites have high content of total REE (ΣREE = 241.99–354.80 μg/g). Chondrite-normalized REE patterns of the biotite plagiogranite have HREE concave-upward shapes and are characterized by the general absence of a significant Eu anomaly with δEu ($\delta Eu = 2Eu_N/(Sm_N + Gd_N)$) ranging from 0.84 to 0.89 (Fig. 4). The tonalites show $(La/Yb)_N = 22.18–29.51$ and $Yb = (0.74–1.20) \times 10^{-6} < 1.8 \times 10^{-6}$. Primitive mantle-normalized element concentration diagrams of the biotite plagiogranite show significant negative anomalies of Nb-Ta, P, K, Th and Ti in conjunction with a positive anomaly of Ba and Sr (Fig. 5), $Sr = (704.61–1\,052.81) \times 10^{-6}$, $Y = (7.17–9.68) \times 10^{-6}$ and high Sr/Y (80.74–281.41). On Sr/Y versus Y (Fig. 6(a)) and $(La/Yb)_N$ versus Yb_N (Fig. 6(b)) diagrams, the Guangtoushan biotite plagiogranites mainly fall within the adakite field.

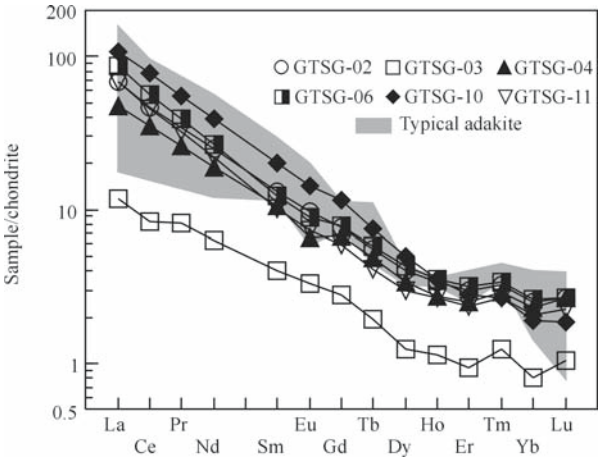

Fig. 4 Rare earth element chondrite-normalized distribution patterns of Guangtoushan granite
Normalized values are from Sun and McDonough (1989). Pattern of typical adakite is from Zhang et al. (2001)

5 Discussion

5.1 Petrogenesis of the Guangtoushan biotite plagiogranites

Compared with the normal I-type granitoids (White and Chappell, 1977), the Guangtoushan biotite plagiogranites display the following characteristics: depleted in Y ($Y = (7.17–9.68) \times 10^{-6} < 18 \times 10^{-6}$) and HREE, enriched in Sr ($Sr = (704.61–1\,052.81) \times 10^{-6}$), Ba with weak positive Sr anomaly in primitive mantle-normalized trace element patterns (Fig. 4), high La/Yb and Sr/Y (80.74–281.41), without significant negative Eu anomalies. These geochemical signatures are comparable to adakites as defined by Defant and Drummond (1990). As shown in Sr/Y-Y and $(La/Yb)_N$-Yb_N diagrams (Fig. 6(a) and (b)), all samples plot in the adakite field. On the SiO_2 versus $(La/Yb)_N$ diagram (Fig. 7), they display different evolution trends with the typical adakites, indicating a unique petrogenesis.

Although the genesis of adakitic magma is still a matter of debate, it is generally accepted that they were derived from sources of basaltic compositions and the presence of significant amounts of garnet ± amohibole is required at some stage in the petrogenesis of these magmas, either as a residual or an early crystallizing assemblage (Condie, 2005; Garrison and Davidson, 2003; Martin, 1999; Martin et al., 2005; Prouteau et al., 2001; Rapp et al., 1999). Petrogenetic models for these magmas possibly formed by partial melting of (1) subducted oceanic slab (Beate et al., 2001; Defant and Drummond, 1990; Gutscher et al., 1999; Peacock et al., 1994; Sajona

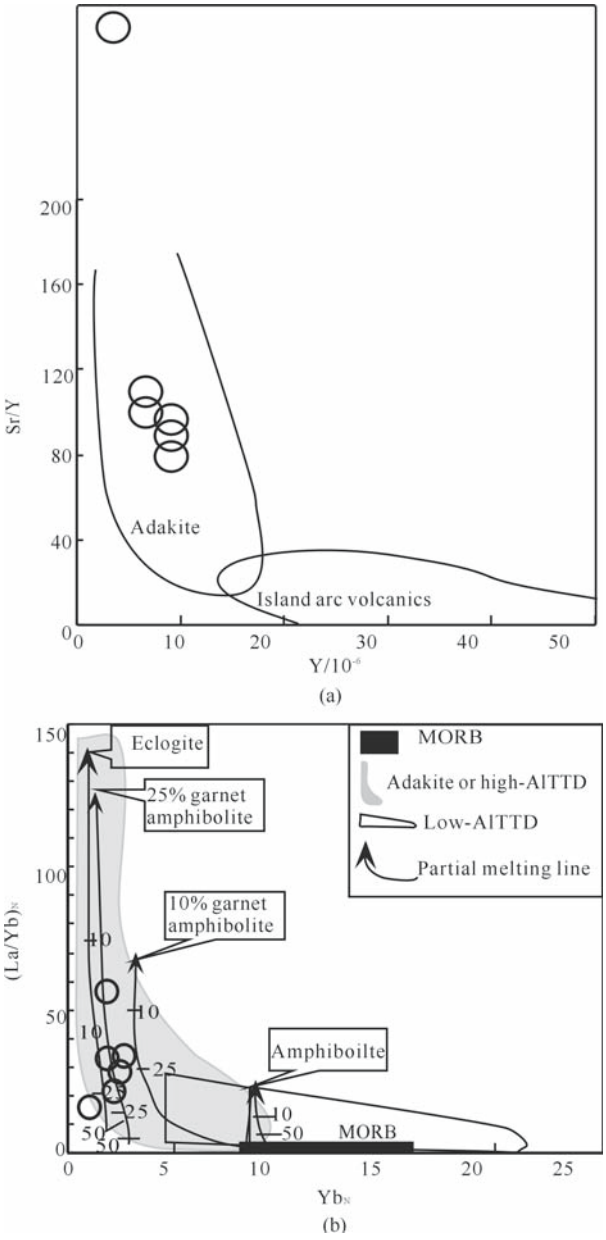

Fig. 6 Y-Sr/Y (a) and Yb_N-$(La/Yb)_N$ (b) diagrams for Guangtoushan granite
Note: Field of adakite is from Defant and Drummond (1990).

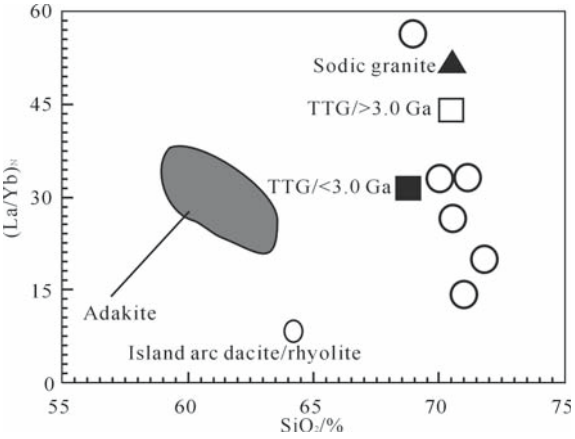

Fig. 7 The SiO_2-$(La/Yb)_N$ diagrams for the Guangtoushan biotite palgiogranite
Notes: The adakite and island arc volcanic field in SiO_2-$(La/Yb)_N$ is cited from Defant and Drummond, 1990; Martin, 1999; Smithes, 2000).

et al., 2000), (2) underplating basaltic lower crust (Atherton and Petford, 1993; Petford and Atherton, 1996), and (3) delaminated lower crust (Gao et al., 2004; Wang et al., 2006; Xu et al., 2002) or thickened lower crust (Chung et al., 2003). Experimental studies show that the magma source for adakite resulted from a basaltic source transformed to garnet amphibolite and/or amphibole eclogite under pressure is equivalent to a thickness of >50 km (Rapp et al., 1995; Sun and Dunnt, 1994).

However, zircon U-Pb dating indicates that the Guangtoushan biotite plagiogranites formed at about 216 Ma (Sun et al., 2002), and the Mianlue Ocean closure, i.e. the Indosinian collision of Yangtze and the North China blocks, occurred at $\sim$242 Ma (e.g. Li et al., 1996), while subduction of Mianlue oceanic crust beneath North China had ceased. Furthermore, the biotite plagiogranites contain more K_2O than adakites from the circum-Pacific belt (Wu et al., 2002). The Guangtoushan biotite plagiogranites have less Mg# (27.5–39.4 < 47) and no negative Eu anomalies, so it can be assumed that they were not derived from fractional crystallization of hydrous basaltic magma or partial melting of deliminated lower crust (Gao et al., 2004). Chondrite-normalized rare earth element patterns are characterized by high ratios of $(La/Yb)_N$, concave-upward shapes of the HREE and lack of significant Eu anomalies. In conjunction with large amounts of Ba and Sr as well as small amounts of Y and HREE, these patterns suggest that the Guangtoushan biotite plagiogranites were formed by partial melting of thickened lower crust (>50 km) with feldspar-poor, garnet $\pm$ amohibole-rich fractionation mineral assemblage in its source region.

5.2 Tectonic implication

Given that the Guangtoushan biotite plagiogranite was produced by partial melting of thickened lower crust, what mechanism can account for their petrogenesis? It is widely accepted that Triassic collision between South China and North China blocks (e.g. Lai et al., 2004; Li et al., 1996; Zhang et al., 2002) might cause the crust in the Qinling orogenic belt and nearby area to be thickened (>50 km). Based on chronology study, Sun et al. (2002) proposed that the Indosinian granites in the South Qinling orogenic belt is syn-collisional, which was formed by the collision between the South China and North China blocks. However, some new evidences suggest that the Guangtoushan pluton is post-collisional. First, according to regional geology, the post-collisional tectonic setting may be an alternative for the formation of the Guangtoushan pluton, because local shear zones observed within the pluton may either represent

late-stage convergent or extensional movements. Second, homochronous post-collisional adakitic granites were identified by Qin et al. (2005).

Thus, it can be concluded that the Guangtoushan adakitic granites can be summarized as follows: Triassic collision between South China and North China blocks caused the subducting slab to break off at very low depth along the Qinling orogenic belt (Davies and von Blanckenburg, 1995), which disturbed the asthenosphere greatly, then the thickened lower crust was extensively heated by mantle-derived mafic magmas and led to the formation of Guangtoushan adakitic granites.

Acknowledgements This work was jointly supported by the National Natural Science Foundation of China (Nos. 40572050, 40272042 and 40234041) and the Teaching and Research Award Program for Outstanding Young Teachers in Higher Education Institutions of MOE, China.

References

Atherton M P, Petford N (1993). Generation of sodium-rich magmas from newly underplated basaltic crust. Nature, 362: 144–146

Beate B, Monzier M, Spikings R, et al (2001). Mio-Plioeene adakite generation related to flat subduction in southern Ecuador: The Quimsaeoeha-oleanic center. Earth and Planetary Science Letters, l92: 499–508

Chung S L, Liu D Y, Ji J, et al (2003). Adakites from continental collision zones: Melting of thickened lower crust beneath southern Tibet. Geology, 31: 1021–1024

Condie K.C (2005). TTGs and adakites: Are they both slab melts? Lithos, 80: 33–44

Davies D W, von Blanckenburg F (1995). Slab breakoff: A model of lithosphere detachment and its test in the magmatism and deformation of collisional orogens. Earth Planet Sci Lett, 129: 85–102

Defant M J, Drummond M S (1990). Derivation of some modern arc magmas by partial melting of young subducted lithosphere. Nature, 347: 662–665

Gao S, Rudnick R L, Yuan H L, et al (2004). Recycling of lower continental crust in the North China craton. Nature, 432: 892–897

Garrison J M, Davidson J P (2003). Dubious case for slab melting in the northern volcanic zone of the Andes. Geology, 31: 565–568

Gutscher M A, Maury R C, Eissen J P, et al (1999). Can slab melting be caused by flat subduction? Geology, 28(6): 535–538

Lai S C, Zhang G W, Dong Y P, et al (2004). Geochemistry and regional distribution of ophiolite and associated volcanics in Mianlüe suture, Qinling–Dabie Mountains. Science in China (Series D), 47: 289–299

Li S G, Sun W D, Zhang G W, et al (1996). Chronology and geochemistry of metavolcanic rocks from Heigouxia Valley in Mianlue tectonic arc, South Qinling: Observation for a Paleozoic oceanic basin and its close time. Science in China (Series D), 39: 300–310

Martin H (1999). The adakitic magmas: Modern analogue of Archean granotoids. Lithos, 46: 411–429

Martin H, Smithies R H, Rapp R, et al (2005). An overview of adakite, tonalite-trondhjemite-granodiorite (TTG), and sanukitoid: Relationships and some implications for crustal evolution. Lithos, 79: 1–24

Peacock S M, Rushmer T, Thompson A B (1994). Partial melting of subducting oceanic crust. Earth and Planetary Science Letters, 121: 227–244

Petford N, Atherton M (1996). Na-rich partial melt from newly underplated basa1tic crust: The Cordmera Blanca Batholith, Peru. Jouma1 of Petrology, 37: 49l–52l

Prouteau G, Scaillet B, Pichavant M, et al (2001). Evidence for mantle metasomatism by hydrous silicic melts derived from subducted oceanic crust. Nature, 410: 197–200

Qin J F, Lai S C, Li Y F (2005). Petrogenesis and geological significance of the Yangba granodiorites from Bikou area, northern margin of Yangtze block. Acta Petrologica Sinica, 21(3): 697–710 (in Chinese with English abstract)

Rapp R P, Shimizu N, Norman M D, et al (1999). Reaction between slab-derived melts and peridotite in the mantle wedge: Experimental constraints at 3.8 GPa. Chemical Geology, 160: 335–356

Sajona F G, Maury R C, Pubellier M (2000). Magmatic source enrichment by slab-derived melts in a young post-collision setting, central Mindanao (Philippines). Lithos, 54: 173–206

Smithes R H (2000). The Archean tonalite-trondhjemite-granodiorite (TTG) series is not an analogue of Cenozoic adakite. Earth and Planetary Science Letters, 182: 115–125

Sun C, Dunn T (1994). Dehydration melting of a basaltic composition amphibolite at 1.5 and 2.0 GPa: Implication for the origin of adakites. Contributions to Mineralogy and Petrology, 117: 394–409

Sun S S, McDonough W F (1989) Chemical and isotopic systemmatics of oceanic basalts: Implication for the mantle composition and process. In: Saunder A D, Norry M J, eds. Magmatism in the Ocean Basins. Geological Society of London Special Publication, 42: 313–345

Sun W D, Li S G, Chen Y D, et al (2002). Timing of synorogenic granotoids in the South Qinling, Central China: Constraints on the evolution of the Qinling–Dabie orogenic belt. Journal of Geology, 110: 457–468

Wang Q, Wyman D A, Xu J F, et al (2006). Petrogenesis of Cretaceous adakitic and shoshonitic igneous rocks in the Luzong area, Anhui Province (eastern China): Implications for geodynamics and Cu-Au mineralization. Lithos, 89: 424–446

White A J R, Chappell B W (1977). Ultrametamorphism and granitoid genesis. Tectonophysics, 43: 7–22

Wu F Y, Ge W C, Sun D Y (2002). The definition, discrimination of adakites and their geological role. In: Xiao Q H, Deng J F, Ma D Q, et al, eds. The Ways of Investigation on Granotoids. Beijing: Geological Publishing House, 172–191 (in Chinese with English abstract)

Xu J F, Shinjio R, Defant M J, et al (2002). Origin of Mesozoic adakitic intrusive rocks in the Ningzhen area of east China: Partial melting of delaminated lower continental crust? Geology, 32: 1111–1114

Zhang B R, Luo T, Gao S, et al (1994). Geochemical Study of the Lithosphere, Tectonism and Metallogenesis in the Qinling-Dabieshan Region. Wuhan: China University of Geosciences Press, 110–122 (in Chinese with English abstract)

Zhang G W, Zhang B R, Yuan X C, et al (2002). Qinling Orogenic Belt and Continental Dynamics. Beijing: Science Press, 1–855 (in Chinese)

Zhang Q, Wang Y, Qian Q, et al (2001). The characteristics and tectonic-metaliogenic significances of the adakites in Yanshan period from eastern China. Acta Petrologica Sinica, 17(2): 236–244 (in Chinese with English abstract)